J. Fluid Mech. (1988), *vol.* 195, *pp.* 1–21
Printed in Great Britain

Aerodynamic focusing of particles in a carrier gas

By J. FERNÁNDEZ DE LA MORA AND P. RIESCO-CHUECA
Yale University, Mechanical Engineering Department, Box 2159 Y.S.,
New Haven, CT 06520, USA

(Received 16 May 1987 and in revised form 11 February 1988)

The problem of whether a stream of microscopic particles may be concentrated into a focal point by entrainment within a carrier gas is considered for dilute particles linearly coupled to the velocity field of an incompressible gas. Typically, the dynamical behaviour of the particles is governed by a so-called Stokes number S, the product of their relaxation time and a characteristic value of the velocity gradient in the suspending fluid. An inequality due to Robinson (1956) is used to illustrate the natural tendency of potential flows to concentrate the particles. For geometries with planar or axial symmetry, with errors cubic in their initial distance to the axis, the trajectories of identical particles originating near an axis of symmetry are shown to cross it at a common focal point provided they have some initial convergence and their Stokes number is larger than a critical value S^*. The position of the focal point of supercritical particles depends on their Stokes number, tending to infinity as S approaches S^*. Particle trajectories originating far from the axis of symmetry are seen to cross the centreline at defocused positions, in analogy with the optical geometric aberration effect. The focusing phenomenon is illustrated numerically for two-dimensional potential flows through nozzles of several geometries and also analysed in the proximity of the axis of symmetry. For these examples, the threshold value S^* of the Stokes number for focusing is of order one, over an order of magnitude larger than typical values of the familiar critical Stokes number marking the onset of particle impaction on solid surfaces. The focal width may be made over two orders of magnitude smaller than the nozzle diameter by restricting the region where particles are seeded to a moderate angle away from the axis. This angle may be higher than $\frac{1}{4}\pi$ for the case of a jet exiting through a slit in an infinitely thin plate. There is also some discussion of the use of high-resolution focusing instruments.

1. Introduction

Under conditions when their Brownian movement may be neglected, the motion of small spherical aerosol particles suspended in a carrier gas may be described through Newton's equation

$$\frac{\mathrm{d}\boldsymbol{u}_\mathrm{p}}{\mathrm{d}t} = -\frac{(\boldsymbol{u}_\mathrm{p}-\boldsymbol{u})}{\tau} + \boldsymbol{g}, \tag{1}$$

where $\boldsymbol{u}_\mathrm{p}$ is the particle velocity, $\boldsymbol{u}$ is the velocity field of the suspending gas, and the force coupling the two has been taken to be linear in the slip velocity $u_\mathrm{p}-u$ through the proportionality constant τ, the particle relaxation time (Friedlander 1977). $\boldsymbol{g}$ is an external acceleration which we shall assume to depend only on position $\boldsymbol{x}$, and to be irrotational. The particle trajectories may thus be determined straightforwardly once τ, $\boldsymbol{g}$ and $\boldsymbol{u}(\boldsymbol{x}, t)$ are specified, together with appropriate injection (initial) conditions for $\boldsymbol{u}_\mathrm{p}$.

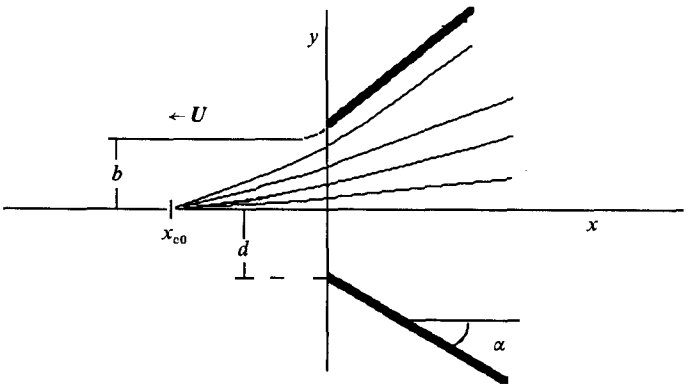

FIGURE 1. Sketch of the aerodynamic focusing scheme. An aerosol suspension is accelerated through a converging nozzle in such a fashion that the particles cross the axis of symmetry at a focal position located at $x = x_{c0}$.

The problem that interests us here is that of concentrating a stream of particles as sharply as possible into nearly a focal point, as schematically shown in figure 1. We shall consider injection conditions such that $\boldsymbol{u}_p = \boldsymbol{u} + \boldsymbol{g}\tau$ in an 'equilibrium' region upstream at infinity, where the derivatives of $\boldsymbol{u} + \boldsymbol{g}\tau$ are negligible. Subsequently $\boldsymbol{g}\tau$ will be absorbed into $\boldsymbol{u}$ without loss of generality, while $\boldsymbol{u}$ is taken as known. The parameter τ in (1) will be treated as a constant and made dimensionless with a characteristic value U of the velocity $\boldsymbol{u}(\boldsymbol{x}, t)$ and a characteristic length L introduced by the geometry of the problem:

$$S = \tau U / L.$$

This group, often called the Stokes number, measures the degree to which $\boldsymbol{u}_p$ and $\boldsymbol{u}$ are uncoupled.

Our problem is then to determine under what conditions (if any) of the function $\boldsymbol{u}(\boldsymbol{x}, t)$ and the Stokes number S an initially uniform distribution of particles can be best made to converge into a focus. The situation differs from that of focusing ions in an electromagnetic field in the dissipative term $-\boldsymbol{u}_p/\tau$ appearing in (1). Also, the driving force is now the velocity field $\boldsymbol{u}(\boldsymbol{x}, t)$ of the carrier gas. For these reasons, we stress the facts that the focusing process is *aerodynamic*, and the particles are *neutral*. The particles may be arbitrarily small, even down to the molecular level, provided their behaviour is approximately deterministic as implied by (1), where Brownian effects are ignored.

Given the practical importance of the brother fields of geometric optics; electron microscopy; mass spectrometry; visible, ultraviolet, X-ray or electron-beam lithography; and so many other areas depending fundamentally on the possibility of bringing photons, ions or electrons into a focus, one can hardly doubt that a systematic investigation on the subject of aerodynamic focusing can be a most rewarding task. From the practical point of view, the perspective of focusing neutral particles adds, to the advantages of traditional ion focusing, the absence of electrostatic repulsion among the particles, so that much denser beams may be contemplated.

Several experimental observations on aerosol focusing have been reported previously. In their pioneering work on high-speed beams of small particles, Israel & Friedlander (1967) noticed that, under some fluid-dynamic conditions, the aerosol

beam entrained in a highly supersonic free jet expanding through a converging nozzle into a low-pressure region was, far from the nozzle, confined to a rather small solid angle (2×10^{-4} sr). Their explanation for this behaviour involved the interplay between the tendency of particles, owing to inertia, to continue their converging flight towards the jet centreline upon exiting a convergent nozzle, counteracted by the tendency of the suspending gas to make their trajectories diverge in the supersonic part of the expansion (figure 1). Most subsequent research on particle focusing has followed this early observation, relying on supersonic jets expanding into highly evacuated regions. An important extension of this early work is due to Israel & Whang (1971), while the most complete characterization available on focusing phenomena in seeded supersonic jets of aerosols is due to Dahneke and his colleagues (Dahneke & Cheng 1979; Dahneke & Hoover 1982; Dahneke, Hoover & Cheng 1982). On the analogous problem where the aerosol particles are substituted by heavy molecules, the limited information available (Fernández de la Mora 1985*a*, *b*) indicates a behaviour similar to that typical of aerosol beams. Nonetheless, no prior experiment has concentrated the seed species into an area significantly smaller than the exit area of the accelerating nozzle.

Subsonic jets of aerosol suspensions have been studied extensively numerically and experimentally (Marple & Willeke 1979; Friedlander 1977), mainly in relation to aerosol-segregating instruments called impactors, where a gas–particle mixture is accelerated through a nozzle and impacted perpendicularly against a flat surface. Particles with a Stokes number larger than a critical value are captured at the surface, while those smaller remain in suspension. To our knowledge, there has been no observation of any focusing effect in such devices; however, the range of the parameter S typical of the operation of aerosol impactors is characteristically constrained to the region around 0.1, the critical value beyond which the particles start impacting on the surface. Furthermore, the exit region of the nozzles used most often in these instruments is not converging but cylindrical, a circumstance likely to reduce any focusing tendency.

The present paper will examine some of the most salient features emerging from an initial analysis of high-resolution aerodynamical focusing. Because the slow progress of this subject can be traced back in part to the considerable difficulties involved in computing accurately the key transonic part of a supersonic expansion (the only flow in which some degree of focusing has been observed thus far), we shall consider incompressible flows principally. Their simplicity will allow the extraction of a number of general conclusions with minor analytical effort. We address basic questions such as whether it is possible to find a velocity field $\boldsymbol{u}(\boldsymbol{x}, t)$ able to focus an aerosol suspension; whether it is preferable to use potential or rotational flows, etc. In particular, we shall find previously unexplored conditions under which a very sharp focus may be attained. Our leading conclusions are summarized in the abstract.

The structure of the paper is the following. First we follow the early work of Robinson (1956) and write an equation for the divergence of the velocity field of the particle phase. The source term is seen to be strictly negative for flows where the symmetrical part of the velocity-gradient tensor dominates over the antisymmetrical (i.e. in potential flows), and positive otherwise. From there it is concluded that rotational flows disfavour focusing. An important inequality (Robinson 1956) establishing that, in potential flows with vanishing initial particle velocity divergence, the particle density always increases along streamlines is illustrated in a

variety of examples. From there it follows that focusing is a quite natural phenomenon rather than a pathology of particle dynamics. Flows constrained by a condition of axial symmetry are considered in §3. A most general finding pertinent to this case arises from an analysis near the axis of symmetry reported in §3.1. The corresponding governing equations are characterized by moving singularities identifiable as focal points, where all trajectories originating in the vicinity of the axis meet. Section 3.2 discusses the special case of linear flows, for which an analytical solution is possible. An infinitely narrow focus may be attained for this problem, for which only particles characterized by a Stokes number larger than a critical value S^* are able to cross the axis and be focused. Off axis, particle trajectories do defocus slightly (in analogy with the so-called geometric optical aberration), in a process that we describe in §§4 and 5. Section 4 explores numerically a limited number of examples of two-dimensional potential flows through nozzles, yielding quantitative predictions on focal distances, critical Stokes numbers and geometric aberration effects as functions of nozzle geometry. A more detailed study of the focal region based on a reduced near-axis form of the governing equations is given in §5. Section 6 discusses some practical aspects of the design of analytical instruments based on aerodynamic focusing. Finally, conclusions are drawn in §7 on some of the findings and the many limitations of this work.

2. Particle piling up: potential versus rotational flows

Whenever their Brownian movement may be neglected, the motion of aerosols in a known fluid flow is governed by Newton's deterministic equation (1). The question is whether the trajectories starting in an upstream region of equilibrium at various spatial locations may be concentrated to the point of crossing each other further downstream at a focus. From similar problems in geometric optics and acoustics it is known that trajectories do often cross each other, being wrapped by singular surfaces called 'caustics' that separate the illuminated from the dark field. That such caustics do also exist in aerosol flows is obvious from considering two perpendicularly opposing jets, one of them being seeded with particles but not the other. The particles from the seeded jet may have enough inertia to penetrate into the originally clean stream, but they are eventually pushed backwards by the opposing flow at a turning point. The envelope of these trajectories is commonly called a caustic, which we shall encounter again in §4. The divergence of the particle velocity field, like their density, goes to infinity at a caustic, where some sort of a partial 'focusing' is achieved.

Subsonic focusing is made possible in principle because the particle phase is not incompressible. It can be compressed by the motion acording to the mass conservation equation

$$\frac{\mathrm{D} \ln \rho_\mathrm{p}}{\mathrm{D}t} = -\nabla \cdot \boldsymbol{u}_\mathrm{p}, \tag{2}$$

because there is no constraint imposing that $\nabla \cdot \boldsymbol{u}_\mathrm{p}$ vanishes. The well-known subsonic feature ensuring incompressibility of gases results from the fact that the molecular motion is fast compared with the mean convective speed, so that the random molecular agitation can readily fill any region of local low density. But particles have a negligible Brownian motion. They are thus highly supersonic with respect to their own thermal speed, and accordingly highly compressible (Fernández de la Mora 1982). It is also posible to predict the direction in which ρ_p changes by considering

the sign of $\nabla\cdot\boldsymbol{u}_p$, thanks to a most notable and neglected study by Robinson (1956). Rewriting the Eulerian form of (1) for the particles,

$$\frac{\partial \boldsymbol{u}_p}{\partial t}+\boldsymbol{u}_p\cdot\nabla\boldsymbol{u}_p\equiv\frac{D\boldsymbol{u}_p}{Dt}=-\frac{(\boldsymbol{u}_p-\boldsymbol{u})}{\tau}, \tag{3}$$

taking its divergence and realizing that $\nabla\cdot\boldsymbol{u}=0$, results in

$$\frac{D\nabla\cdot\boldsymbol{u}_p}{Dt}+\frac{\nabla\cdot\boldsymbol{u}_p}{\tau}=-l, \tag{4}$$

where

$$l\equiv\frac{\partial u_{pi}}{\partial x_j}\frac{\partial u_{pj}}{\partial x_i},$$

and summation with respect to repeated subindices is implicit. Robinson (1956) extended Kelvin's circulation theorem to the $\boldsymbol{u}_p$ field, so that if $\boldsymbol{\omega}_p=\nabla\times\boldsymbol{u}_p$ vanishes far upstream and $\nabla\times\boldsymbol{u}=0$ throughout the flow field, then $\boldsymbol{\omega}_p$ also vanishes everywhere. Indeed, the velocity $\boldsymbol{\omega}_p$ of the particles obeys the equation

$$\frac{D\boldsymbol{\omega}_p}{Dt}+\boldsymbol{\omega}_p\nabla\cdot\boldsymbol{u}_p-\boldsymbol{\omega}_p\cdot\nabla\boldsymbol{u}_p=\frac{\nabla\times\boldsymbol{u}-\boldsymbol{\omega}_p}{\tau},$$

implying that, when $\boldsymbol{\omega}_p=0$ initially, it can only grow driven by the vorticity $\nabla\times\boldsymbol{u}$ of the carrier fluid. Because l is always positive for the case of irrotational flows, (4) may be integrated to prove that $\nabla\cdot\boldsymbol{u}_p$ is always negative or null if it vanishes far upstream. Robinson's (1956) inequality follows

$$\frac{D\rho_p}{Dt}>0, \tag{5}$$

and there is a tendency for particles to pile up as they move along streamlines. The extension of Robinson's analysis to rotational flows is straightforward. By decomposing the velocity-gradient tensor $\partial u_{pi}/\partial x_j$ into its symmetrical and antisymmetrical parts $\boldsymbol{e}$ and $\boldsymbol{\Omega}$, respectively, l may be written as

$$l=(\boldsymbol{e}+\boldsymbol{\Omega}):(\boldsymbol{e}-\boldsymbol{\Omega})=\boldsymbol{e}:\boldsymbol{e}-\boldsymbol{\Omega}:\boldsymbol{\Omega}=\boldsymbol{e}:\boldsymbol{e}-\tfrac{1}{4}\boldsymbol{\omega}_p\cdot\boldsymbol{\omega}_p. \tag{6}$$

Accordingly, the contribution of $\boldsymbol{\omega}_p$ to l is strictly negative, tending to decrease the rate of growth of ρ_p along streamlines, opposing the process of streamline convergence and thus delaying or cancelling focusing effects. Therefore, because the only external source for $\boldsymbol{\omega}_p$ is $\nabla\times\boldsymbol{u}$, one can immediately say that focusing will be favoured whenever $\nabla\times\boldsymbol{u}=0$ and disfavoured (though not necessarily stopped) otherwise. It is tempting to attribute these defocusing effects to the centrifugal forces associated with local vorticity. However, because centrifugal forces can arise in irrotational as well as rotational flows (see figure 2), it is clear that they can lead to either focusing or defocusing.

Equation (5) is a powerful statement. It is a sort of second law saying that the final equilibrium state of an aerosol moving in a potential flow approaches the focused state of infinitely concentrated particles. And this concentrating tendency has nothing to do with coagulation or interparticle attraction; it is a purely dynamical result of the motion inside the carrier fluid. Obviously, since the overall particle mass is conserved, the fact that ρ_p increases along particle streamlines is compensated by the creation of vacuum or dust-free regions where no particle trajectory reaches. Such a particle tendency to pile up in some regions and to evacuate others completely

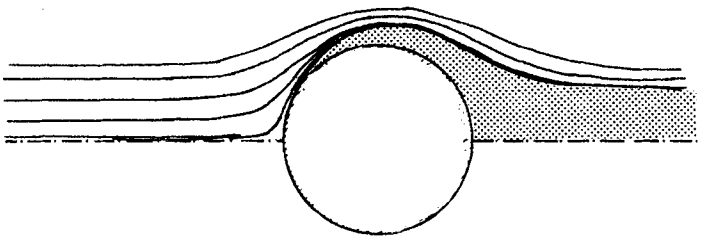

FIGURE 2. Qualitative sketch of particle streamlines in a potential flow around a cylinder for a value of the Stokes number near the critical one for impaction onset. The only particle trajectory intercepting the cylinder is the stagnation line, which is tangent to it. This particle streamline 'separates' from the cylinder, leaving a 'wake' where no particles may reach. The creation of this 'vacuum' is compensated by an increase in concentration along particle streamlines according to Robinson's inequality (5). Notice the significant piling up of particles near the limit trajectory.

is illustrated in figure 2 for the well-known problem of potential flow about a circular cylinder of radius R moving at speed U_∞ in an otherwise undisturbed fluid (Batchelor 1977). Under the condition shown, when $\tau U_\infty/R = \frac{1}{8}$, the cylinder has concentrated a large amount of dust close to the 'vacuum interface'. It thus appears that focusing is a most natural feature of potential flows.

It is interesting to note that the phenomenon of particle impaction also tends to be favoured in irrotational flows, at least for the case of linear flows where the fluid velocity-gradient tensor is spatially uniform (Fernández de la Mora 1985*a*, *b*).

3. On the existence of focal-point singularities

Designing a focusing nozzle is a typical example of the inverse problem often facing the aerodynamicist. Given the nozzle shape one can determine the flow field and the particle trajectories. But, what is the nozzle shape, if any, that will bring an aerosol stream into a focus? In the present section we prove that focal-point singularities may actually exist for some flow fields, first through a near-axis analysis in situations with planar or axial symmetry, and then by considering an exactly solvable problem.

3.1. *Eulerian analysis near an axis of symmetry*

An axially symmetric geometry will provide a stringent constraint on the motion of the particles, thus strongly enhancing their natural tendency to concentrate. Accordingly, although non-symmetric geometries might be of interest, we shall now consider two- or three-dimensional nozzles with planar or axial symmetry. In order to be focused, the particles must obviously cross the axis where any existing focal point is constrained to lay. It is, thus, most natural to attempt a local description in the proximity of the axis, in analogy with the so-called paraxial or Gaussian limit of geometric optics. Under such conditions, one may prove very generally the possible existence of focal points.

Let u, v, u_p and v_p be the fluid and particle velocities parallel and perpendicular to the axis of symmetry, and let x and y be the coordinates parallel and perpendicular to the axis. We consider two-dimensional as well as axisymmetric flow fields. In the proximity of the axis ($y = 0$), with errors of order y^2 for u and of order y^3 for v, we may write

$$u = u(x), \tag{7}$$

$$v = y\beta(x), \tag{8}$$

where, under steady-state conditions, the functions $u(x)$ and $\beta(x)$ are related through the mass conservation equation

$$(n+1)\beta+\frac{\mathrm{d}u}{\mathrm{d}x}=0,$$

in which n is unity for axisymmetric and zero for two-dimensional flows. The particles are originally in equilibrium with the fluid ($\boldsymbol{u}_\mathrm{p}=\boldsymbol{u}$ far upstream), so that the injection conditions are compatible with a solution of the form

$$u_\mathrm{p}=u_\mathrm{p}(x), \tag{9}$$

$$v_\mathrm{p}=y\beta_\mathrm{p}(x). \tag{10}$$

Hence the steady-state particle momentum conservation equations (3) become the ordinary differential equations

$$\tau u_\mathrm{p}u_\mathrm{p}'+u_\mathrm{p}-u=0, \tag{11}$$

$$\tau(u_\mathrm{p}\beta_\mathrm{p}'+\beta_\mathrm{p}^2)+\beta_\mathrm{p}-\beta=0, \tag{12}$$

where primes denote differentiation with respect to x. The first of these expressions is uncoupled from the second, and merely determines the particle velocity along the axis. For all reasonably conceived nozzle shapes, u_p will be a smooth function of x, certainly free from zeros or singularities. The information of greatest interest is contained in the equation for β_p, whose quadratic term β_p^2 is capable of producing singularities where β_p diverges. These are called moving singularities because the coefficients of the ordinary differential equation are not themselves singular, and because the point x_0 at which β_p diverges (or not) depends on the boundary conditions and other parameters of the problem such as τ. That (12) does indeed admit an explosive behaviour may be shown by realizing that, close to the hypothetical singularity, the term $\beta_\mathrm{p}-\beta$ can be neglected compared with β_p^2, leading to the following solution:

$$\beta_\mathrm{p}^{-1}=\frac{\int^x \mathrm{d}x}{u_\mathrm{p}}. \tag{13}$$

Clearly, β_p can diverge as $1/(x-x_0)$ at particular points x_0 whose exact location must be determined numerically, and which depend on τ and the specific form of $u(x)$ (that is, on particle size and fluid flow field). A singularity of β_p must be interpreted as a focal point, because the particle trajectories are given by the separable equation

$$\beta_\mathrm{p}y/\mathrm{d}y=u_\mathrm{p}/\mathrm{d}x, \tag{14}$$

with solution

$$y=\frac{A\exp\int^x \beta_\mathrm{p}(x)\,\mathrm{d}x}{u_\mathrm{p}(x)}, \tag{15}$$

where A is a constant taking a different value for each particle trajectory. From the exponential form of (15) y cannot possibly vanish (crossing the axis) for a finite value of x unless β_p diverges (remember that u_p has no zeros). But if β_p diverges at a particular point x_0, y vanishes independently of the value of A and thus independently of the particular streamline considered. Therefore, we make the remarkable inference that, if one particle trajectory crosses the axis, all trajectories near the centreline also cross through exactly the same focal point. And the present result has very broad generality, because no assumption on the fluid flow is made

except for that of symmetry. The same conclusions would hold for rotational and viscous flows (of course, the vorticity vanishes at the axis), and also if a more complicated nonlinear expression were to be used for the drag law coupling the particles to the gas in (1). The extension of these results to compressible flows is also straightforward and only requires to take into account the variation of τ with pressure and temperature.

The above theoretical conclusion on the existence of foci will be confirmed numerically in §4 (and analytically in §3.2 for a rather special situation) with the additional observation that particles below a critical size, characterized by a value of the Stokes number of order unity, $S^* = O(1)$, never cross the centreline, while supercritical particles converge at an axial focal point whose position depends on $S(\tau)$, tending to infinity as S tends to S^*.

3.2. *The case of linear flows*

The case of flows in which $\boldsymbol{u}(\boldsymbol{x})$ is linear with the position vector $\boldsymbol{x}$ is particularly interesting, because, when written in Lagrangian form in terms of $\boldsymbol{x}$ and its derivatives, (1) becomes a set of exactly solvable linear ordinary differential equations with constant coefficients. This situation is a special limit of (9) and (10), except that their validity is not now restricted to small values of y and that β is now a constant, $-\beta_0$. Accordingly, if the initial particle velocity v_p is linear with y at an injection surface $x =$ constant, where u_p is independent of y, then all particle trajectories will cross the axis at exactly the same location, independently of their initial proximity to it: there is no geometrical aberration for this class of flows. Furthermore, the underdamped–overdamped transition associated with the equation of motion in the y-direction

$$\frac{\tau \, \mathrm{d}^2 y}{\mathrm{d}t^2} + \frac{\mathrm{d}y}{\mathrm{d}t} + \beta_0 y = 0$$

occurs when the group $\tau\beta_0$ (the Stokes number S for this problem) takes the value $\frac{1}{4}$, corresponding to the threshold condition when particles start crossing the axis and thus become focused. This behaviour is exactly analogous to that of particles approaching the stagnation point in front of an obstacle in an inviscid fluid (Friedlander 1977). In that case, supercritical particles start impacting on the obstacle, while in the present one they start crossing the axis of symmetry. Hence, the phenomenon of particle focusing is also characterized by a critical value S^* of the Stokes number.

4. Focal parameters and geometric aberration in two-dimensional potential flows

Several features of the focusing phenomenon seen above may be illustrated and a few new ones identified after examination of the particle flow field in some examples. Those described below are chosen from among the relatively restricted family of potential flows in two-dimensional problems. The triple assumption (incompressibility, irrotationality and two-dimensionality) is not satisfied in most physical situations, but the qualitative conclusions of our analysis may be extended to more general flows. In the absence of an analytical specification of the gas velocity field a numerical description becomes necessary.

Let (x, y) again be the coordinates along and perpendicular to the axis. The complex potential is defined as $\omega = \phi + \mathrm{i}\psi$, where ϕ is the velocity potential and ψ

the stream function. The geometry is specified by the lines of constant ψ after supplying a relation between ω and $z = x + iy$ (hence the velocity is $v = (\mathrm{d}\omega/\mathrm{d}z)^*$ where the superscript * denotes the complex conjugate).

In the first example, the flow through a hyperbolic two-dimensional nozzle is considered and approximately modelled through the relation (Milne-Thomson 1938) $z = \sinh\omega$ or $v^* = (z^2+1)^{-\frac{1}{2}}$, with streamlines $y^2/\sin^2\psi - x^2/\cos^2\psi = 1$. Lengths have been normalized using the distance $2L_0$ between the two branch-point singularities at $z = \pm\mathrm{i}$ where $|v|$ tends to infinity. Velocities are made dimensionless by means of the centrepoint speed U_0. In order to confine the particles to the near-axis region where a sharp focus may be expected (§3.1), the nozzle region is bounded by two symmetrical streamlines $\pm\psi_0$ (in our numerical example $\psi_0 = 0.3746$ rad). Each trajectory is characterized by the value of ψ on the fluid streamline from which it originates in the region far upstream.

In the units just defined, (1) becomes

$$\boldsymbol{u}_\mathrm{p}\cdot\nabla\boldsymbol{u}_\mathrm{p} = -\frac{(\boldsymbol{u}_\mathrm{p}-\boldsymbol{u})}{S}, \tag{16}$$

where $\boldsymbol{u}_\mathrm{p}$ is the unknown particle velocity and $\boldsymbol{u}$ is the carrier-gas velocity field. $S = \tau U_0/L_0$ is taken to be 4 in this example, roughly equal to twice the critical value S^* below which there is no centreline crossing. The resulting trajectories are shown in figure 3, with a sharp focal region located around $x = 1.61$. One can see, upon closer examination of the numerical results, that the particles are concentrated in a region some 100 times smaller than the throat diameter. As predicted in §3.1, such a clean-cut focus is a consequence of the relatively small values used for ψ_0. But the situation deteriorates progressively for trajectories originating at larger angles away from the axis because, whenever ψ is not small, a phenomenon analogous to the optical geometric aberration effect may shift significantly the point of axial crossing.

For small values of ψ, the particle trajectories cross the axis at a position indistinguishable from the singular points of (11) and (12). The axial coordinates of these singular points are shown in figure 4 as a function of the Stokes-number parameter S. Notice again the existence of a critical value S^* at which the focus tends to infinity and below which no focusing occurs.

A more realistic complex potential model can be used to describe the outflow from a symmetrical nozzle with straight walls (figure 1): an open-ended two-dimensional internal wedge with half-angle α (Milne-Thomson 1938; Batchelor 1977). The relation between the final jet width $2b$ and the orifice width $2d$ is called the contraction ratio $\beta = b/d$. An explicit relation z *vs.* ω is not available for an arbitrary value of α, but the physical and potential planes are mapped through a differential equation

$$\mathrm{d}z/\mathrm{d}\omega = \exp(-\tfrac{1}{2}\pi\omega) + \{1+\exp(-\pi\omega)\}^{\frac{1}{2}}]^{2\alpha/\pi}. \tag{17}$$

The normalization velocity and length are chosen to be the final jet velocity U and half-width b (see figure 1). Equation (17) is complemented with the boundary condition

$$z = z_0 = \mathrm{i}\beta \quad \text{for } \omega = \omega_0 = \mathrm{i}.$$

An Euler integration scheme of (17) along a suitable path in the complex plane z linking z_0 to the destination point provides a direct relation $\omega(z)$. By itself, (17) gives a direct representation of the velocity field $\boldsymbol{u}$ in terms of the complex potential ω. It

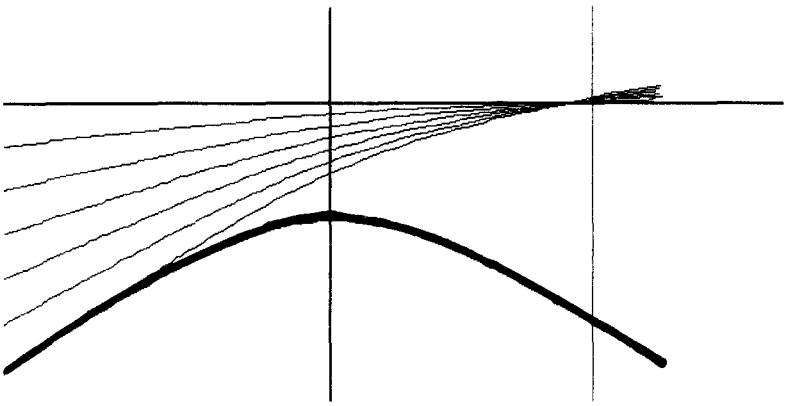

FIGURE 3. Sketch of the particle trajectories inside a hyperbolic nozzle with an asymptotic semiangle of convergence of 22°. The Stokes number is 4 in the units of (16).

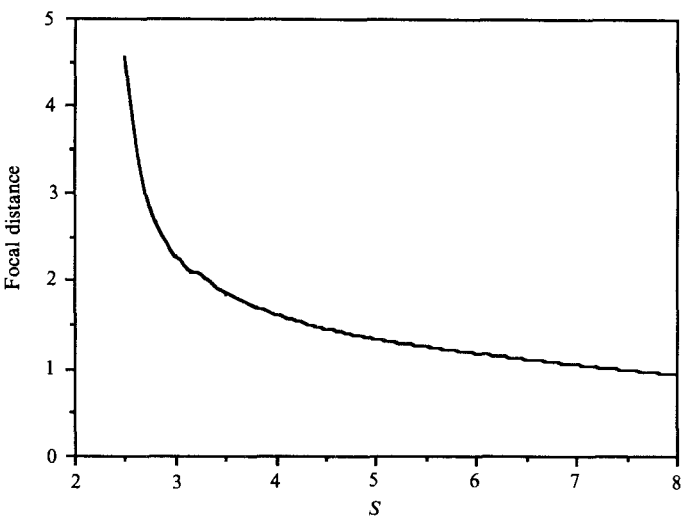

FIGURE 4. Focal distance x_{c0}/L_0 as a function of particle Stokes number for two-dimensional potential flow through a hyperbolic nozzle.

is therefore convenient to carry out the integration of Newton's equation (16) in the complex potential plane, using (ϕ, ψ) as alternative coordinates rather than (x, y):

$$\frac{\mathrm{d}\omega_\mathrm{p}}{\mathrm{d}t} = \boldsymbol{u}_\mathrm{p}\frac{\mathrm{d}\omega}{\mathrm{d}\varkappa} = \boldsymbol{u}_\mathrm{p}\boldsymbol{u}^*, \tag{18}$$

$$\frac{\mathrm{d}\boldsymbol{u}_\mathrm{p}}{\mathrm{d}t} = \frac{\boldsymbol{u}-\boldsymbol{u}_\mathrm{p}}{S}, \tag{19}$$

and then relating ω and $\varkappa$ through the above-mentioned Euler integration. This model supplies an excess of information which needs to be simplified by synthetizing the main featurs of the focal region into a few representative parameters. The centreline-crossing point x_c depends in general on the location where the particle trajectory originates. That is, x_c is a function of the initial stream function ψ_0 at the streamline where the particles are seeded. The shape of the dependence $x_\mathrm{c}(\psi_0)$,

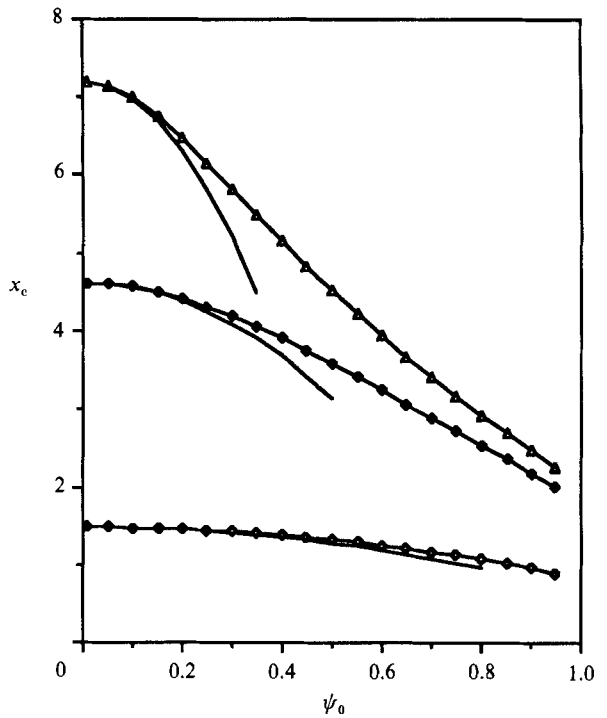

FIGURE 5. Crossing point x_{c0}/L_0 as a function of seeding stream function ψ_0 for $S = 8$ (◇), 2.25 (◆) and 2.05 (△), in the flat-plate-orifice nozzle ($\alpha = \frac{1}{2}\pi$) outlet flow.

whose nature will be further investigated in the next section, is displayed in figure 5 for the case of an orifice in a flat plate ($\alpha = 90$) and different values of the Stokes number, defined for this example as $S = U\tau/b$. Two important features characterize each curve $x_c(\psi_0)$. One is the curvature at the origin $A = \{d^2x_c/d\psi_0^2\}_{\psi=0}$ which measures the amount of geometric aberration; the other is x_{c0}, the virtual focus location in the absence of aberration, $x_{c0} = x_c(0)$. A double pattern can clearly be noticed in the figure: as S decreases, x_{c0} increases. Eventually a threshold value of S (the critical Stokes number S^*) will be reached where $x_{c0} \to \infty$, below which only particle trajectories originating far from the axis might eventually cross the centreline. As the critical Stokes number is approached, the sharpness of the focus decreases and A grows indefinitely.

The virtual-focus location x_{c0} is plotted in figure 6 as a function of S for different values of α, as a criterion for comparing different nozzle shapes. It is clear from the figure that all the curves have a vertical asymptote corresponding to the critical Stokes number, as well as a horizontal asymptote resulting from the limit of infinite inertia (when $S \gg 1$, the streamlines are radial, centred at a point located at a distance $x_{c0} = d/\tan\alpha$ from the nozzle outlet). It can also be observed that the critical Stokes number grows considerably with decreasing α.

Figure 7 gives additional insight into the problem by showing the profile of different streamlines (all of them originating in the positive ψ_0) at the focal region for the case $\alpha = \frac{1}{2}\pi$. The trajectories, which differ in slope and crossing point depending on the value of $\psi_0 \approx \theta_{\text{initial}}/\alpha$, determine an envelope (boundary of the dust-free region, or caustic) where the particle density peaks singularly before dropping to zero in the outside dust-free layer. As pointed out earlier, caustics are a common feature

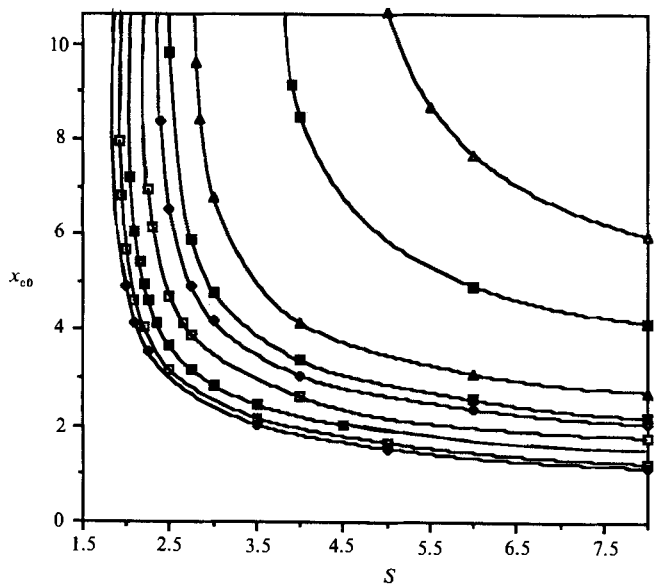

FIGURE 6. Crossing point x_{c0}/L_0 for initial stream function tending to zero as a function of the Stokes number $S = U\tau/b$ for different wedge half-angle α in the two-dimensional conical nozzle flow: $\alpha = \pi/8$ (△), $\pi/6$ (■), $\pi/4$ (▲), $3\pi/10$ (■), $\pi/3$ (◆), $2\pi/5$ (⊡), $\pi/2$ (■), $3\pi/5$ (□), $2\pi/3$ (◆).

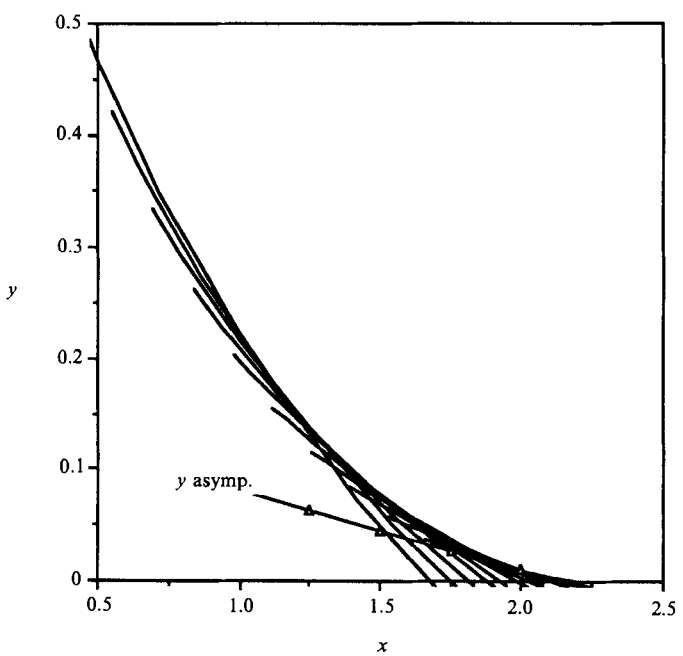

FIGURE 7. Particle streamlines originating from the upper half-plane in the two-dimensional conical nozzle flow ($\alpha = \frac{1}{2}\pi, S = 4$). Also represented is the envelope calculated asymptotically.

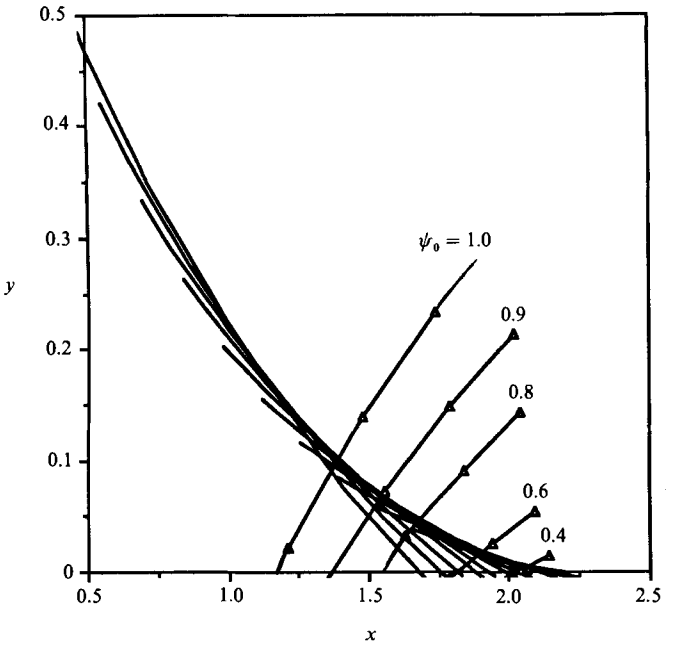

FIGURE 8. Focal region for the same case as in figure 7 showing caustic, emerging trajectories (with $\psi_0 = 0.4$, 0.6, 0.8, 0.9 and 1 respectively) and particle jet throat.

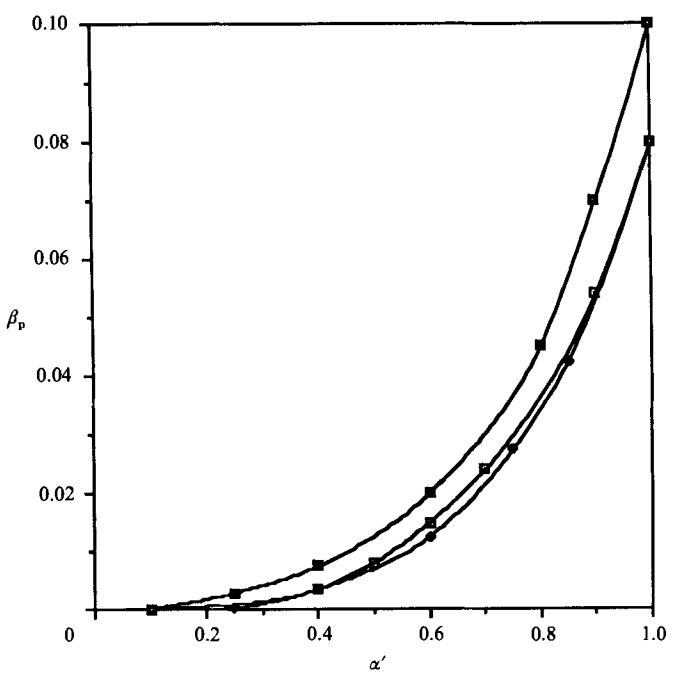

FIGURE 9. Particle jet contraction rate β_p as a function of the seeding angle α' in a two-dimensional conical nozzle flow ($\alpha = \frac{1}{2}\pi$) for different Stokes numbers: $S = 2.05$ (⊡), 2.25 (◆) and 4 (■).

of systems where the evolution of a field is given by solving ordinary differential equations along characteristic lines, and they represent a sort of partial condensation of a three-dimensional space into a surface. When the caustic merges with the axis, a stringent symmetry condition condenses further the singular surface into a line, the axis itself. Foci may thus arise as the points of tangency between caustics and the axis of symmetry.

The picture is complicated by the presence of streamlines originating with negative ψ_0 which, after crossing the centreline at a given point $x_c(\psi_0)$ will emerge in the other half-plane and cross the caustic line. The first negative $-\psi_0$ trajectory to cross the caustic determines the minimum radius containing all the particles or particle jet throat whose location (x_t, y_t) depends on the upstream injection conditions. Consider for instance the case where particles are seeded in a range of angles from α' to $-\alpha'$, i.e. $|\psi_0| < \psi_{0\,\mathrm{lim}} = \alpha'/\alpha$. It is clear from figure 8 that the throat precedes the virtual focus or apex of the caustic. Maximal densities are to be expected at the virtual focus while the maximum contraction rate of the full particle jet takes place at the throat ($\beta_p \equiv y_t/d$). As α' decreases, β_p decreases. Focusing can thus be seen to be favoured by large nozzle angles α and moderate seeding angles α'. Figure 9 shows that even when $\alpha = \alpha'$, in the case of a flat plate with an orifice ($\alpha = \frac{1}{2}\pi$), the contraction rate stays below 10% for a variety of Stokes numbers.

If a plate were inserted normally to the flow, the shape of the expected deposits that one would see could be inferred from the particle streamline profiles shown in figure 7. For $x < x_t$ all the deposit would be confined within the sharply marked boundary corresponding to the caustic. Between x_t and x_{c0} the caustic is encircled by a fainter halo produced by emergent particles after crossing the centreline. For $x > x_{c0}$, there is no caustic and the deposit becomes gradually fainter away from the centre.

5. Near-axis description of the focal region

In §3, a preliminary Eulerian analysis supplied a straightforward illustration of the existence and location of moving singularities identified as foci. This procedure is limited in that it is not easy to refine beyond lowest order and therefore is not informative about geometric aberration. These higher-order phenomena are treated in this section by a near-axis Lagrangian analysis.

5.1. *Near-axis expansion for problems with a complex potential* ω

In two-dimensional problems with planar symmetry, assuming the existence of a complex potential, it is possible to carry out a systematic expansion to yield an asymptotic description of the focal region. Let $\psi_0 \ll 1$ be the seeding stream function far upstream for the trajectory under consideration. Taking into account the symmetry, the position and velocity of the particles can be expressed in powers of $\epsilon = \psi_0$:

$$\phi = \phi_0 + \epsilon^2\phi_1 + \ldots, \quad \psi = \epsilon(\gamma_0 + \epsilon^2\gamma_1 + \ldots),$$

$$u = u_0 + \epsilon^2 u_1 + \ldots, \quad v = \epsilon(v_0 + \epsilon^2 v_1 + \ldots),$$

while similar expansions can be used to express the carrier-gas velocity $\boldsymbol{u}$:

$$u_l = u_{l0} + \epsilon^2 u_{l1} + \ldots, \quad v_l = \epsilon(v_{l0} + \epsilon^2 v_{l1} + \ldots).$$

Hence, after using (18) and (19), one obtains the following set of equations:

$$u_0' = \frac{u_{l0}-u_0}{S}, \quad u_1' = \frac{u_{l1}-u_1}{S}, \tag{20}$$

$$v_0' = \frac{v_{l0}-v_0}{S}, \quad v_1' = \frac{v_{l1}-v_1}{S}, \tag{21}$$

$$\phi_0' = u_0 u_{l0}, \qquad \phi_1' = u_1 u_{l0} + v_0 v_{l0} + u_0 u_{l1}, \tag{22}$$

$$\gamma_0' = v_0 u_{l0} - u_0 v_{l0}, \quad \gamma_1' = v_1 u_{l0} + v_0 u_{l1} - u_0 v_{l1} - u_1 v_{l0}, \tag{23}$$

where $\mathrm{d}/\mathrm{d}t$ is symbolized by a prime. The above is a system of ordinary differential equations for the unknown velocity and location of the particles. The location of the virtual focus will be given by the value of ϕ_0 at the point where $\gamma_0 = 0, \phi_{c0} = \{\phi_0\}_{\gamma_0=0}$. The dependence of the crossing point as a function of ϵ can be expressed as the expansion

$$\phi_c(\epsilon) = \phi_{c0} + \epsilon^2 \phi_{c1} + \ldots, \tag{24}$$

where ϕ_{c1} is a measure of the geometric aberration and can be shown to be

$$\phi_{c1} = \phi_1 - \gamma_1 \left(\frac{\mathrm{d}\gamma_0}{\mathrm{d}\phi_0}\right),$$

where the right-hand side is evaluated at ϕ_{c0}. Hence

$$x_c = x_{c0} + \epsilon^2 x_{c1} + \ldots, \tag{25}$$

where $x_{ci} = \phi_{ci}(\mathrm{d}x/\mathrm{d}\phi)$ (also evaluated at ϕ_{c0}); for instance, in the case of a flat-plate nozzle ($\alpha = \frac{1}{2}\pi$), for i = 1, 2, ...:

$$x_{ci} = \phi_{ci}\{\exp(-\tfrac{1}{2}\pi\phi_{c0}) + [1+\exp(-\pi\phi_{c0})]^{\frac{1}{2}}\}^{2\alpha/\pi}.$$

Equation (25) is compared to the result from a direct integration of (18) and (19) in figure 5. The good agreement observed indicates that (20)–(23) provide a simple means to determine the amount of geometric aberration. Additionally, these equations contain some information about the local description of streamlines at the focus, where they can be approximated as straight lines:

$$y = (x - x_c)\tan\theta,$$

where both the slope $\tan\theta$ and the crossing point x_c depend on the value of the initial stream function ψ_0. Accordingly

$$\tan\theta = \epsilon(m_{c0} + \epsilon^2 m_{c1} + \ldots),$$

where $m_{c0} = v_{c0}/u_{c0}$ and $m_{c1} = m_{c0}(v_{c1}/v_{c0} - u_{c1}/u_{c0})$ (the c-subindex indicates that the v_i and u_i are evaluated at ϕ_{c0}). Thus

$$y = \epsilon\{m_{c0}(x-x_{c0}) + \epsilon^2[m_{c1}(x-x_{c0}) - m_{c0}x_{c1}] + \ldots\} = f(x,\epsilon). \tag{26}$$

The family of curves $f(x,\epsilon)$ gives rise to an envelope (caustic) obtained from the intersection of $y - f(x,\epsilon) = 0$ with $\partial f/\partial\epsilon = 0$:

$$y_e = \pm 4 m_{c0}(x-x_{c0})\tfrac{1}{3}\{m_{c0}\tfrac{1}{3}(x-x_{c0})[m_{c0}x_{c1} - m_{c1}(x-x_{c0})]\}^{\frac{1}{2}} + O(x-x_{c0})^2. \tag{27}$$

Equation (27) is plotted in figure 7, where it is seen to compare rather well with the actual envelope in the vicinity of the axis. One interesting result from (27) is that the initial slope of the caustic at the focus x_{c0} is null since $y_e \sim |x-x_{c0}|^{\frac{3}{2}}$. The throat can

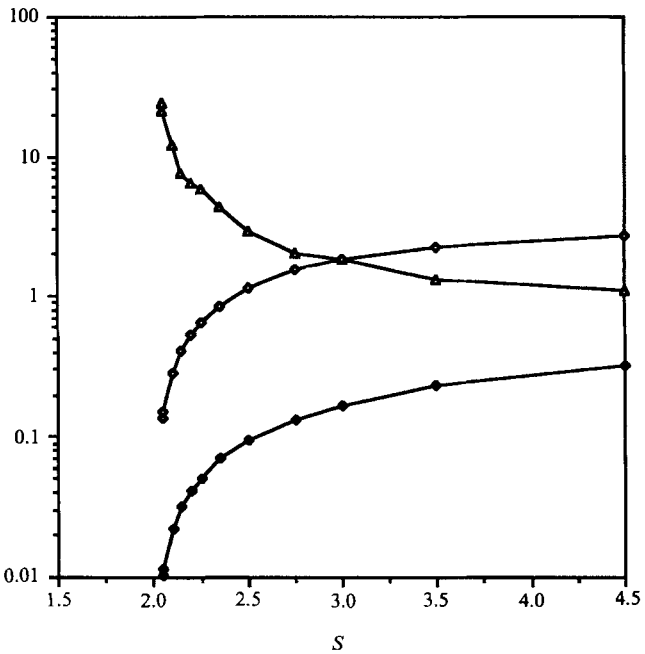

FIGURE 10. Geometric-aberration parameter x_{c1} (△) and crossing-angle factors $-m_{c0}$ (◆) and m_{c1} (◇) for the case of a flat-plate-orifice nozzle ($\alpha = 90$) as a function of the Stokes number S.

be located as the intersection of (27) with $f(x, \psi_{\lim})$. The root of the corresponding system of nonlinear equations can be determined by Newton's method.

The parameters x_{c0} (virtual-focus location), x_{c1} (geometric aberration) and m_{c0}, m_{c1} (streamline slope at crossing point) are therefore sufficient to give a good description of the focal region. Figure 10 gives the x_{c1}, m_{c0} and m_{c1} profiles for the case of a flat-plate-orifice nozzle ($\alpha = 90$) as a function of the Stokes number S.

In conclusion, the near-axis analysis yields a very simple access to the essential parameters describing the focal region.

5.2. *General near-axis expansion for axisymmetric or two-dimensional problems*

Let us characterize a particle trajectory by means of the value of the fluid stream function ψ at which particles are seeded in the fluid upstream at infinity. ψ is rescaled in such a way that it becomes unity on the boundary of the nozzle and vanishes on the centreline, so that $\psi \ll 1$ in the vicinity of the axis. We further define $\epsilon = \psi^{1/n}$, where $n = 1$ for two-dimensional and 2 for axisymmetric problems. Accordingly, the particle streamline is

$$y = y(t, \epsilon), \quad x = x(t, \epsilon), \tag{28}$$

which may be expanded in powers of ϵ as

$$y = \epsilon y_0(t) + \epsilon^3 y_1(t) + \ldots, \tag{29}$$

$$x = x_0(t) + \epsilon^2 x_1(t) + \ldots. \tag{30}$$

Analogously

$$u_p = u_0(t) + \epsilon^2 u_1(t) + \ldots, \tag{31}$$

$$v_p = \epsilon v_0(t) + \epsilon^3 v_1(t) + \ldots. \tag{32}$$

In order to expand Newton's equation (1) for the particles in powers of ϵ we first expand the fluid velocity field in powers of y and then in powers of ϵ by means of (29) and (30):

$$u(x,y) = U_0(x) + y^2 U_1(x) + \ldots \tag{33}$$

$$= U_0(x_0 + \epsilon^2 x_1 + \ldots) + \epsilon^2 (y_0 + \epsilon^2 y_1 + \ldots)^2 U_1(x_0 + \epsilon^2 x_1 + \ldots) + \ldots$$

$$= U_0(x_0) + \epsilon^2 \{x_1 U_0'(x_0) + y_0^2 U_1(x_0)\} + O(\epsilon^4), \tag{34}$$

where the definitions of U_0, U_1 etc., are implicit in (17), and primes denote derivatives with respect to x_0. Analogously

$$v(x,y) = y V_0(x) + y^3 V_1(x) + \ldots \tag{35}$$

$$= \epsilon V_0(x_0)\, y_0 + \epsilon^2 \{y_1 V_0(x_0) + y_0 x_1 V_0'(x_0) + y_0^3 V_1(x_0)\} + O(\epsilon^4). \tag{36}$$

We now write Newton's equations for the particles in Lagrangian coordinates, using primes for the time derivatives acting on lower-case variables (but still denoting derivatives with respect to x_0 by primes acting on V_i and U_i),

$$\tau u' + u - U(x,y) = 0, \quad \tau v' + v - V(x,y) = 0, \tag{37}$$

$$x' = u_p, \quad y' = v_p. \tag{38}$$

Expanding in powers of ϵ by means of (29)–(32), (34) and (36) one obtains at the two leading orders:

$$\tau u_0' + u_0 - U_0(x_0(t)) = 0, \tag{39}$$

$$\tau v_0' + v_0 - V_0(x_0(t)) = 0, \tag{40}$$

$$\tau u_1' + u_1 - \{x_1(t)\, U_0'(x_0(t)) + y_0^2(t)\, U_1(x_0(t))\} = 0, \tag{41}$$

$$\tau v_1' + v_1 - \{y_1 V_0 + y_0 x_1 V_0' + y_0^3 V_1\} = 0, \tag{42}$$

$$x_0' = u_0; \ldots, \quad x_n' = u_n, \tag{43}$$

$$y_0' = v_0; \ldots, \quad y_n' = v_n. \tag{44}$$

The initial conditions for the case when particles are injected upstream at infinity in an equilibrium region where the gradients of $\boldsymbol{u}(\boldsymbol{x}, t)$ vanish are that $\boldsymbol{u}_p = \boldsymbol{u}$ and that the particle trajectories coincide with a fluid streamline: the kinematics and the dynamics of both phases are identical. Knowing the fluid velocity field $u(x,y), v(x,y)$, by means of the relations $\mathrm{d}t = \mathrm{d}x/u = \mathrm{d}y/v$, one may obtain expressions

$$y = y(t,\epsilon), \quad x = x(t,\epsilon) \tag{45}$$

which may be expanded exactly as (29) and (30) for the particles providing explicit expressions for the x_i, y_i. These may be used as initial conditions to start the integration of (43) and (44). The initial conditions for the u_i and v_i result from ignoring the primed terms multiplied by τ in their corresponding dynamical equations (39)–(42).

6. Some practical considerations on particle focusing instruments

The present paper has examined some of the most salient features emerging from an initial analysis on the subject of high-resolution aerodynamical focusing. Because such a singular phenomenon might be the basis for new instruments capable of

concentrating and size-separating particles, some discussion on their potential and limitations will be worthwhile.

6.1. *On the smallest particle size that can be focused*

In order to be focused, a particle must have a Stokes number larger than a critical value S^*, which depends on the geometry and the fluid-dynamical conditions. For a given particle size, S may be increased by increasing the flow velocity and by decreasing the gas pressure and the nozzle diameter. The upper limit for the velocity in a converging nozzle is the speed of sound, while the pressure and nozzle diameter can only be reduced at the expense of decreasing the nozzle Reynolds number. Because of the negative effects of the vorticity generated within the viscous regions near the nozzle walls, it is unlikely that Reynolds numbers much below a few hundreds might yield good focusing results. Accordingly, there is a definitive limit to the smallest particle size that can be focused. To extend that range one would have to design transonic nozzles with the smallest possible value of S^* and capable of performing adequately within a range of moderate Reynolds numbers. The challenge to the aerodynamicist is thus very considerable. But the analytical advantages of focusing sharply ultrafine particles and macromolecules might well deserve the effort. A look at figure 6 indicates that a very substantial reduction in S^* may be achieved by using wide angles of convergence. A similar phenomenon arises in highly supersonic axisymmetric jets, for which, after increasing the half-angle of a conical nozzle from 15° to 90°, we have recently measured a value of S^* nearly an order of magnitude smaller than that found by Dahneke *et al.* (1982). This substantial improvement makes it possible to focus molecules with molecular masses of several hundred atomic units seeded in He or H_2, a situation that we are currently exploring experimentally.

6.2. *On the limits to the focal sharpness attainable*

Geometric aberration is a limitation that can in principle be overcome by appropriate aerodynamic design. Even in the unlikely event that the aerodynamical analogue of a broad field lens were to be unattainable, geometric aberration phenomena could be eliminated by simply seeding the particles only in the region near the axis. This procedure was successfully followed by Dahneke *et al.* (1982) and has the additional advantage of eliminating possible defocusing effects originating in the viscous regions near the nozzle walls.

Perhaps a more serious problem would result from the singularity of the phenomenon itself, by virtue of which the particle concentration diverges at the focal point. As a result, one might be obliged to consider particle–particle collisions and coagulation phenomena in the vicinity of the focus, which might result in a focal-region structure with a finite width even for trajectories originating in the neighbourhood of the axis. Nonetheless, it is clear that the importance of this hypothetical difficulty will decrease with particle dilution. Furthermore, the problem is self-alleviated because the main purpose of focusing is concentrating and there seems to be no need to concentrate highly a suspension that is not highly dilute to start with.

A most important limiting factor on the focusing sharpness for very fine aerosols and heavy molecules is Brownian motion, which inevitably spreads out each particle streamline. In fact, the above description in terms of deterministic Newtonian trajectories parallels rather well classical geometric optics and its equally deterministic 'rays'. And, as in its optical diffraction analogue, the inclusion of Brownian motion within the picture complicates rather dramatically the theoretical

formulation. When the Stokes number is not a small parameter the standard equations of diffusion are not applicable, and the problem must be dealt with within a kinetic rather than a hydrodynamic framework. A good measure of the defocusing effects of Brownian motion is the inverse of a Mach number based on the particle convective velocity and its speed of thermal agitation, a quantity too minute to be of any concern for high-speed flows except perhaps in the rather interesting region of ultrafine particles and macromolecules.

6.3. *On the effect of a collecting surface*

Our computations of §4 involved various jets, none of which was intercepted by a collecting surface. The free-jet geometry is of interest for analytical instruments where various particle sizes are differentially focused along the jet centreline, and counted non-intrusively. However, other particle-size spectrometers may be based on collecting the focused beam on a surface, or on sampling it through a small centred hole for further analysis. In that case, the flow field is modified by the collecting or collimating surfaces, as are the particle trajectories. Consequently, our curves of focal distance as a function of S would have to incorporate the nozzle-to-plate distance L as an additional parameter. The information of greatest practical interest would be a curve representing, for every value of L, the corresponding value of the Stokes number of the particle whose focal point falls right on the collecting surface or on the middle of the collimating hole. In principle, such a curve could be quite different from those shown in figure 6. However, the circumstance that the critical Stokes number for focusing is much larger than that required for impact on a surface (typically 0.1 or 0.2) implies that a particle large enough to focus in the absence of a collecting plate will have more than sufficient inertia to be affected only slightly by the presence of the plate. On that basis, it seems reasonable to expect that our figure 6 will not be too different from the hypothetical figure mentioned above which accounted for the presence of the plate. This rough approximation is even more precise in the case of highly supersonic flows, where the loss of stagnation pressure in the shock wave ahead of the obstacle and its small separation from the surface make the Stokes number for impact considerably larger than that characteristic of the nozzle-exit region, the one relevant for focusing (Fernández de la Mora 1985*a*).

7. Summary of results and limitations of this work

The limited amount of initial explorations carried out above on the subject of aerodynamic focusing seems to indicate that:

(i) Potential flows lead to the concentration of particles, thus favouring focusing. Rotational flows appear to have the opposite effect.

(ii) The focus is infinitely sharp in a hypothetical linear flow in which particle trajectories may be found analytically and where only particles with a Stokes number greater than $\frac{1}{4}$ manage to cross the axis.

(iii) The focus is infinitely sharp in symmetrical nozzles for the streamlines near the axis of symmetry.

(iv) There is a 'geometrical aberration' that defocuses slightly the streamlines originating far from the jet centreline. In spite of it, numerical examples show that the width of the focal region may be made over two orders of magnitude smaller than the nozzle diameter by restricting the region where particles are seeded to a moderate angle away from the axis. This angle may be higher than $\frac{1}{4}\pi$ for the case of a jet exiting through a slit in an infinitely thin plate.

(v) Focusing occurs only for particles characterized by a value of the Stokes number greater than a critical value S^*, which is typically of order unity.

(vi) The focus is rather sharp except perhaps near critical conditions, under which the focal point tends to infinity and geometric-aberration effects appear to be singular. For that reason, high-resolution focusing might be easier to attain at finite distances from the source. This observation might explain why previous aerosol-beam experiments (where the collecting surface was invariably hundreds of nozzle diameters downstream from the source) only achieved a modest degree of focusing.

(vii) Because the spatial location of the singularity depends on τ, by collecting particles at varying axial positions one would create a particle mass spectrometer of great sensitivity and separation power.

However, many of these findings are limited by a variety of mechanisms not considered in our idealized examples. Important but non-limiting factors are viscous phenomena on the nozzle walls, turbulent mixing at the boundary of the free jet, the effects of a collecting surface placed on the path of the jet, fluid compressibility, the nonlinearity of the drag law connecting the two phases, etc. Diffusion appears as a most important limiting factor on the focusing sharpness for very fine aerosols and heavy molecules.

A study of the effects of vorticity and of non-symmetric geometries or initial conditions will very likely enrich the limited range of situations analysed here, as hinted in a most interesting work on the motion of particles and bubbles in a two-dimensional cellular flow which has appeared while this manuscript was being reviewed for publication (Maxey 1987). This paper finds a broad range of conditions where all the trajectories of both the particles and the bubbles merge asymptotically into a few special accumulation planes. In addition to providing another rather striking example of the tendency of particles to concentrate singularly in some privileged regions, Maxey's work is interesting in that it illustrates the phenomenon for a strongly rotational flow field as well as finding accumulation surfaces which do not always (but sometimes) coincide with planes of symmetry of the fluid flow. Maxey covers conditions in some ways broader than those considered here; but he explores only one moderately small value of the Stokes number at which no foci arise. Nonetheless, because his accumulation curves are most likely dependent on S, they suggest another promising approach for designing analytical instruments capable of discriminating between different particle sizes while simultaneously concentrating each of them.

This paper is dedicated to the memory of K. T. Whitby. We are indebted to Dogan Günes (Istanbul) to R. Fernández-Feria, D. E. Rosner, S. Cohen and S. Fuerstenau (Yale) for useful discussions. This research has been supported by the National Science Foundation, Grant CBT-8612143 and the U.S. Department of Energy Grant DE-FG02-87ER13750.

REFERENCES

BATCHELOR, G. K. 1977 *An Introduction to Fluid Dynamics*. Cambridge University Press.

BORN, M. & WOLF, E. 1959 *Principles of Optics*. Pergamon.

DAHNEKE, B. E. & CHENG, Y. S. 1979 *J. Aerosol Sci.* **10**, 257–274.

DAHNEKE, B. E. & HOOVER, J. 1982 In *Rarefied Gas Dynamics* (ed. S. S. Fisher) AIAA.

DAHNEKE, B. E., HOOVER, J. & CHENG, Y. S. 1982 *J. Colloid Interface Sci.* **87**, 167.

FERNÁNDEZ DE LA MORA, J. 1982 *Acta Mech.* **43**, 261–265.

FERNÁNDEZ DE LA MORA, J. 1985*a* *J. Chem. Phys.* **82**, 3453–3464.

FERNÁNDEZ DE LA MORA, J. 1985*b* *Aerosol Sci. Technol.* **4**, 339–349.

FRIEDLANDER, S. K. 1977 *Smoke, Dust and Haze*, Section 4.6. Wiley.

ISRAEL, G. W. & FRIEDLANDER, S. K. 1967 *J. Colloid Interface Sci.* **24**, 330–337.

ISRAEL, G. W. & WHANG, J. S. 1971 Dynamical properties of aerosol beams. *Tech. Note* BN-709. Institute for Fluid Dynamics and Applied Mathematics, University of Maryland.

MARBLE, F. E. 1970 *Ann. Rev. Fluid Mech.* **2**, 397.

MARPLE, V. A. & WILLEKE, K. 1979 Inertial impactors. In *Aerosol measurements* (ed. D. A. Lundgren, F. S. Harris, Jr., W. H. Marlow, M. Lippmann, W. E. Clark & M. D. Durham), pp. 90–106. University of Florida Press.

MAXEY, M. R. 1987 *Phys. Fluids* **30**, 1915–1928.

MILNE-THOMPSON, L. M. 1938 *Theoretical Hydrodynamics*, Macmillan.

ROBINSON, A. 1956 *Commun. Pure Appl. Maths* **IX**, 69–84.